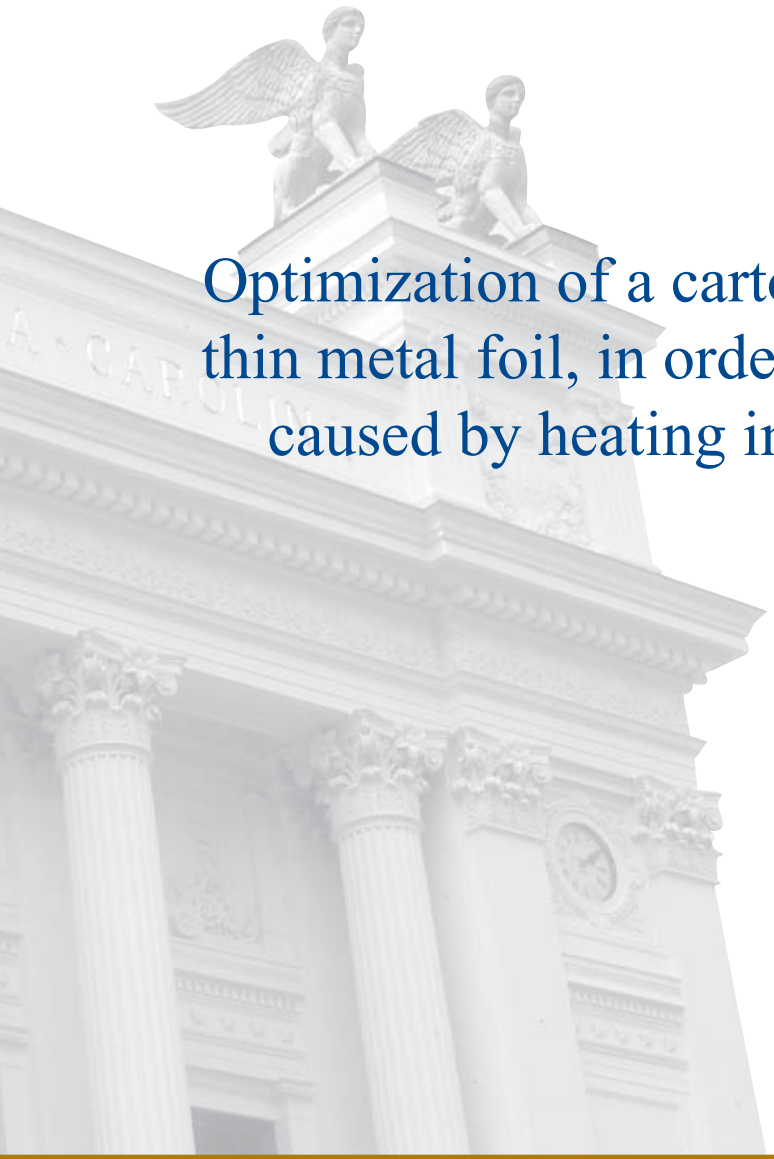

Optimization of a carton package containing thin metal foil, in order to prevent ionization caused by heating in a microwave oven

Master of Science Thesis
Tomas Barregård & Pär Ström
in cooperation with
Tetra Recart AB
December 2004

Department of Electroscience

LUND
UNIVERSITY

Abstract

It is possible to manufacture a cardboard package equivalent to a tin by adding a thin metal foil. This kind of package has the advantages of being light, easy to shelf and requiring limited space when disposed of.

This master thesis investigates the possibilities to heat a Tetra Recart carton containing a thin foil of metal, in a microwave oven. There is a problem when used in a microwave oven since the metal foil causes ionization. Distinct flashes appear from two specific parts of the carton after a short time inside the oven.

To investigate the problem with ionization a Finite-Difference Time-Domain (FTDT) model was made in the program SEMCAD. In order to find a solution, the properties that cause ionization have been investigated by literature studies and experimental tests. The problem with ionization is related to accumulation of the electric field at sharp edges. Ionization can be completely prevented by minor changes of the carton.

Acknowledgements

We would like to thank our supervisors Eva Jonsson and Bengt Andersson at Tetra Recart for all the support while doing this master thesis project. We would also like to thank our supervisor Anders Karlsson at the Department of Electroscience in Lund for all his help.

Table of contents

1 Introduction

1.1 The problem in brief

Tetra Recart is a company within the Tetra Pak group with the aim to produce packages equivalent to a tin. The packages are made of cardboard, plastic and a thin metal foil. The difficulties to use metal objects in a microwave oven is known by most people. Despite that, Tetra Recart is interested in making their carton safe to heat in microwave ovens.

This master thesis investigates the possibilities to use a Recart carton in a microwave oven operational at the frequency 2.45 GHz. The carton contains a thin foil of metal protecting the food from the surrounding atmosphere. There is a problem when the carton is heated in a microwave oven, since the metal foil causes ionization.

When the problem was presented a comprehensive planning was suggested. It consisted of the following parts, in chronologic order:

- Computer simulations of a carton heated in a microwave oven
- Verification of simulations through experimental tests
- Suggesting solutions
- Verification of solutions with computer simulations
- Verification of solutions with experimental tests

The used approach is quite similar to the suggested planning, with the exception that all suggested solutions have been verified with experimental test rather than by computer simulations. The computer simulations have been made with the Finite-Difference Time-Domain (FTDT) program SEMCAD. Instead of only suggesting and testing possible solutions to the problem a few test cases have been treated to find the properties that are relevant for ionization.

1.2 The carton

The primary object that has been tested and evaluated is the Tetra Recart 400 ml standard carton (TRC 400), which is shown in figure 1.1. The carton is fabricated from a laminate of paper, plastic and a thin foil of aluminium in several different layers and is a totally retortable package. Our focus is on the aluminium since it has the ability to work as an antenna for microwave frequencies. The aluminium has benefits in this sort of packages as a barrier against air and light and it works as a heat surface when sealing the carton with induction. When investigating ionization some parts of the carton are critical. These parts are the folding at the bottom and the top edge where the carton is ripped open, see figure 1.2.

Figure 1.1. Ordinary 400 ml cartons. These cartons are easy to shelf due to their shape.

In this report, parts of the carton have been given specific names. The folding is shown in figure 1.3, where the *Triangles* and the *Bottom fold edge* are visible. *Triangles* refer to the two triangular parts of the folding. *Bottom fold edge* is the edge that connects the triangle parts and is partly hidden by them.

Figure 1.2. Carton being ripped open along the perforation at the top.

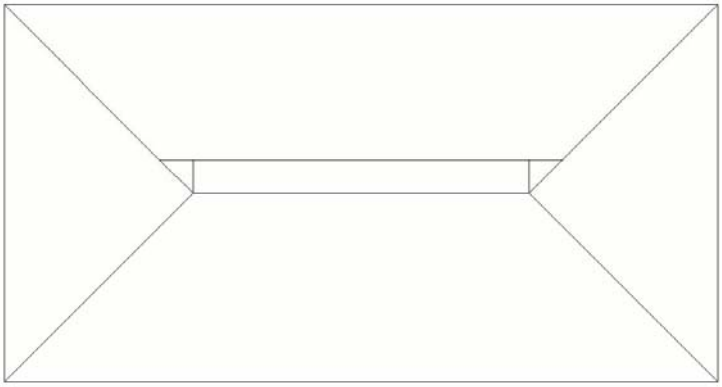

Figure 1.3. This picture shows the way the bottom is folded on an ordinary carton. The triangles and the bottom fold edge are visible.

1.3 Guide to reading this report

In chapter 2 some theory is presented for the electromagnetic fields, the computational method, heating and ionization. It gives an overview of the theory that is related to this thesis and gives examples of literature for extensive studies. The methods used in this thesis have been divided into chapter 3 and chapter 4, experimental methods are treated in chapter 3 and computational methods in chapter 4. The results are presented in chapter 5, these results and the methods mentioned earlier are discussed in chapter 6. The conclusions that can be made are summarized in chapter 7. At the end of this report references can be found as well as appendices for calculations and pictures. Appendix E contains a list of symbols for quantities that are used in the equations in this thesis.

2 Theory

2.1 Computational methods

There are mainly three different mathematical methods for computing electromagnetic phenomena in a computer. One of these methods is called Method of Moment (MoM) and is not commonly used to calculate scattering of waves. The remaining two methods are called Finite Element Method (FEM) and Finite-Difference Time-Domain (FDTD). Both of these two methods can be used for simulations of the fields heating a carton in a microwave oven. The most obvious difference between FDTD and FEM is the way volumes are represented in the grid. In common FDTD-programs a three-dimensional grid consists of cuboids and in the FEM case tetrahedrons are used.

2.2 Advantages and disadvantages with FDTD

The FDTD method has a great advantage to FEM when it comes to calculation speed. The explicit nature of FDTD requires less computational resources compared to FEM, when solving a three-dimensional problem with $n \times n \times n$ cells. FEM is an implicit method that requires matrix inversions. Depending on the technique used to find inverse matrices the order of the computational time and the required storage space can be compared in table 2.1 (Risman 2000). The information used during calculation is preferably stored in the computer memory.

	Memory usage	Computational time
FDTD	n^3	n^4
FEM (direct)	n^5	n^7
FEM (iterative)	n^3	between n^4 and n^6

Table 2.1. Required memory and time for solving a problem for different computational methods. Only the orders of the values are given, the grid consists of $n \times n \times n$ cells.

Thin objects that are not aligned with the axes and non cubic objects like spheres will result in a poor discretization, since the grid consists of rectangular cubic cells. The easiest way to reduce this error between the model and the grid is to alter the overall cell size. Since that greatly increases the simulation time other alternatives are currently at work. One alternative is to use a subgrid to increase the resolution locally in the critical zone. This option will be implemented in the not yet released SEMCAD V2.0 (http://www.semcad.com/solver_enhancements.html).

In several applications, including simulation of microwave ovens, it is of interest to study a band of frequencies. With the usage of a transient pulse source a single FDTD simulation can compute results for multiple frequencies, only requiring an additional Fourier transformation to be made. That is much more efficient than FEM which would have to run a complete simulation for each frequency.

2.3 Electromagnetic fields

Maxwell's equations play an important part in all field theory. The equations are called Faraday's law, Ampère's law, Poisson's equation and the condition of solenoidal magnetic field and are viewed as equation 2.1-2.4. In Faraday's law the magnetic current density **M** has been added. Adding the magnetic conductivity gives a duality between Faraday's law and Ampère's law. However one should remember that a non-zero magnetic current is impossible since magnetic charge does not exist.

$$\nabla \times \mathbf{E} = -\frac{\partial \mathbf{B}}{\partial t} + \mathbf{M} \tag{2.1}$$

$$\nabla \times \mathbf{H} = \frac{\partial \mathbf{D}}{\partial t} + \mathbf{J} \tag{2.2}$$

$$\nabla \cdot \mathbf{D} = \rho \tag{2.3}$$

$$\nabla \cdot \mathbf{B} = 0 \tag{2.4}$$

It is natural to assume that the involved materials are linear, isotropic and nondispersive. That assumption is valid for a wide range of materials and it is a criterion for the constitutive relations in equation 2.5 and 2.6. The constitutive relations in combination with Maxwell's equations can be used to derive an FDTD-algorithm. This is done with great detail in Taflove (2000) and is presented briefly in chapter 2.4 of this report.

$$\mathbf{D} = \varepsilon_{\mathrm{r}} \cdot \varepsilon_0 \cdot \mathbf{E} \tag{2.5}$$

$$\mathbf{B} = \mu_{\mathrm{r}} \cdot \mu_0 \cdot \mathbf{H} \tag{2.6}$$

Fields behave in a specific way close to conductive surfaces. For a perfect electric conductor (PEC) the electric field is normal to the surface and the magnetic field is tangential to the surface. This behaviour can be derived from Maxwell's equations as boundary conditions.

2.4 FDTD-algorithm

Equation 2.7 and 2.8 can be created by substitution of equation 2.5 and 2.6 into equation 2.1 and 2.2. Equation 2.7 and 2.8 are often called Maxwell's curl equations and can be used to predict variations of fields in time, given only the initial fields and current densities. The current densities can be treated as a combination of current caused by fields and additive sources as in equation 2.9 and 2.10.

$$\frac{\partial \mathbf{H}}{\partial t} = -\frac{1}{\mu_r \cdot \mu_0} \cdot (\nabla \times \mathbf{E}) - \frac{1}{\mu_r \cdot \mu_0} \cdot \mathbf{M} \tag{2.7}$$

$$\frac{\partial \mathbf{E}}{\partial t} = \frac{1}{\varepsilon_r \cdot \varepsilon_0} \cdot (\nabla \times \mathbf{H}) - \frac{1}{\varepsilon_r \cdot \varepsilon_0} \cdot \mathbf{J} \tag{2.8}$$

$$\mathbf{M} = \mathbf{M}_{\text{source}} + \sigma^* \cdot \mathbf{H} \tag{2.9}$$

$$\mathbf{J} = \mathbf{J}_{\text{source}} + \sigma \cdot \mathbf{E} \tag{2.10}$$

If Cartesian coordinates are used equation 2.7 and 2.8 can be divided into three equations each. These new equations can be used to express the time derivative of the size of different vector components as viewed in equation 2.11-2.16. In equation 2.11-2.16 equation 2.9 and 2.10 have been used to divide current densities into different types of currents.

$$\frac{\partial H_x}{\partial t} = -\frac{1}{\mu_r \cdot \mu_0} \cdot \left(\left(\frac{\partial E_y}{\partial z} - \frac{\partial E_z}{\partial y} \right) - \left(M_{\text{source}_x} + \sigma^* \cdot H_x \right) \right) \tag{2.11}$$

$$\frac{\partial H_y}{\partial t} = -\frac{1}{\mu_r \cdot \mu_0} \cdot \left(\left(\frac{\partial E_z}{\partial x} - \frac{\partial E_x}{\partial z} \right) - \left(M_{\text{source}_y} + \sigma^* \cdot H_y \right) \right) \tag{2.12}$$

$$\frac{\partial H_z}{\partial t} = -\frac{1}{\mu_r \cdot \mu_0} \cdot \left(\left(\frac{\partial E_x}{\partial y} - \frac{\partial E_y}{\partial x} \right) - \left(M_{\text{source}_z} + \sigma^* \cdot H_z \right) \right) \tag{2.13}$$

$$\frac{\partial E_x}{\partial t} = -\frac{1}{\varepsilon_r \cdot \varepsilon_0} \cdot \left(\left(\frac{\partial H_z}{\partial y} - \frac{\partial H_y}{\partial z} \right) - \left(J_{\text{source}_x} + \sigma \cdot E_x \right) \right) \tag{2.14}$$

$$\frac{\partial E_y}{\partial t} = -\frac{1}{\varepsilon_r \cdot \varepsilon_0} \cdot \left(\left(\frac{\partial H_x}{\partial z} - \frac{\partial H_z}{\partial x} \right) - \left(J_{\text{source}_y} + \sigma \cdot E_y \right) \right) \tag{2.15}$$

$$\frac{\partial E_z}{\partial t} = -\frac{1}{\varepsilon_r \cdot \varepsilon_0} \cdot \left(\left(\frac{\partial H_y}{\partial x} - \frac{\partial H_x}{\partial y} \right) - \left(J_{\text{source}_z} + \sigma \cdot E_z \right) \right) \tag{2.16}$$

In order to create an algorithm, that calculates the field variations, the time must be divided into steps and the space into cells. Figure 2.1 is an example of how the space can be divided into a mesh. This mesh is often referred to as the Yee space lattice. Note that the field components are denoted in such a way that each E-component is surrounded by four H-components and each H-component is surrounded by four E-components.

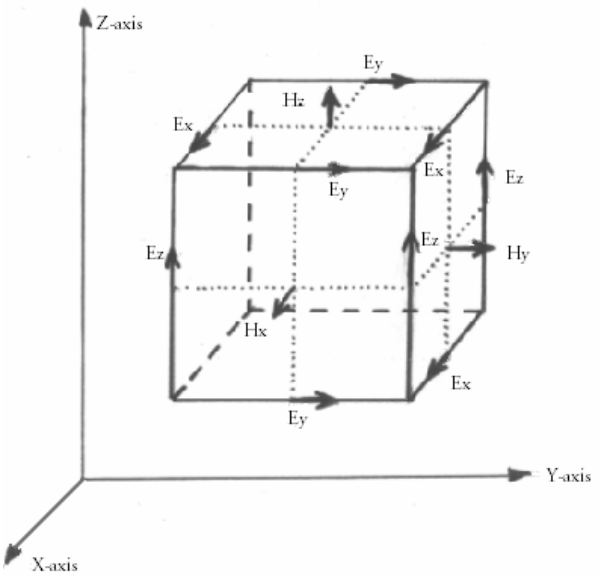

Figure 2.1. Space divided into a cubic mesh based on Cartesian coordinates called the Yee space lattice.

An arbitrary point in the mesh will have the indices i, j, k and n to represent position in the mesh as well as the time step according to equation 2.17. With the same notation the derivatives of time and space can be approximated as in equation 2.18 and 2.19. The approximation in equation 2.20 is useful in order to approximate field strength at unknown time steps.

$$F\big|_{i,j,k}^{n} = F\left(i \cdot \Delta x,\, j \cdot \Delta y,\, k \cdot \Delta z,\, n \cdot \Delta t\right) \tag{2.17}$$

$$\frac{\partial F\big|_{i,j,k}^{n}}{\partial t} \approx \frac{F\big|_{i,j,k}^{n+\frac{1}{2}} - F\big|_{i,j,k}^{n-\frac{1}{2}}}{\Delta t} \tag{2.18}$$

$$\frac{\partial F\big|_{i,j,k}^{n}}{\partial x} \approx \frac{F\big|_{i+\frac{1}{2},j,k}^{n} - F\big|_{i-\frac{1}{2},j,k}^{n}}{\Delta x} \tag{2.19}$$

$$F\big|_{i,j,k}^{n} \approx \frac{F\big|_{i,j,k}^{n+\frac{1}{2}} + F\big|_{i,j,k}^{n-\frac{1}{2}}}{2} \tag{2.20}$$

The equations that have been presented so far in this chapter can be combined into a leap frog algorithm. When the Yee space lattice is chosen the curl equations can be used to calculate both the electric and magnetic fields, given the initial values and the sources. The electric field and the magnetic field are calculated alternating. The calculations require limited usage of memory since only values for the last time step are needed to be saved. The final equations for a leap frog algorithm, based on the derivations in this chapter, are presented in appendix A.

2.5 Stability for FDTD

The grid in FDTD can not be chosen arbitrary. The cubes are not required to have the same size, but there is a limit for the stability and a limit for the high order errors (Bondeson 2002). The requirement for stability limits either the dimensions of the smallest cell or the length of the time step. The condition is written in equation 2.21 where Δt is the time step and $x_{\text{cell min}}$, $y_{\text{cell min}}$ and $z_{\text{cell min}}$ are the dimensions of the smallest cell in the grid.

$$\Delta t = \frac{1}{c} \cdot \frac{1}{\sqrt{\frac{1}{x_{\text{cell min}}^2} + \frac{1}{y_{\text{cell min}}^2} + \frac{1}{z_{\text{cell min}}^2}}} \tag{2.21}$$

In order to limit high order errors the dimensions of the cells should not be large compared to the length of a wave in the material. If the length of a cell is 1/10.5 of a wavelength the error, due to partial cancellation of the spatial and temporal errors in the stability limit, is less than 1% (Bondeson 2002).

2.6 Microwave oven

The most important part of a microwave oven is the magnetron. When a magnetron is supplied with a pulsed DC-voltage it generates electromagnetic waves. The waves are guided through one or more waveguides that feed the microwave cavity. The geometry of all waveguides are chosen in order to support the fundamental mode $TE_{m,n=1,0}$. Except for the cavity, where the object that is to be heated is placed, a microwave oven generally contains different mechanisms to produce a multimode field and support uniform heating. More information about function of microwave ovens can be read in Roddy (1986).

Inside the microwave oven waves generated by the magnetron is directed into the oven cavity through one or more waveguides. The dimension of a square waveguide can be calculated with equation 2.22 and 2.23 (Karlsson 1996). The cut-off frequency given by equation 2.22 should be chosen lower than the microwave frequency (usually 2.45 GHz). The transversal wave number for a rectangular waveguide is given by equation 2.23 (choose $m = 1$ and $n = 0$ for the fundamental mode). a is the longest dimension and b is the shortest dimension.

$$f_{\text{c}} = \frac{k_{\text{t}} \cdot c}{2 \cdot \pi \cdot \sqrt{\varepsilon_{\text{r}} \cdot \mu_{\text{r}}}} \tag{2.22}$$

$$k_{\text{t}_{\text{m,n}}}^2 = \pi^2 \cdot \left(\frac{m^2}{a^2} + \frac{n^2}{b^2} \right) \tag{2.23}$$

2.7 Heating of water

The frequency of a microwave oven is usually 2.45 GHz. That frequency is chosen to give both maximum heating and uniform heating. Water molecules are dipoles, which allow dipole relaxation. The depth of penetration in water is sufficiently long compared to the size of food objects. Hence absorption and dielectric loss due to dipole relaxation are the two main contributions to the heating of water at microwave frequencies. Both of these effects are close to optimum at 2.45 GHz. Microwave heating is sometimes incorrectly explained as resonance of water molecules, but this occurs at much higher frequencies.

2.8 Wavelength and depth of penetration

In the investigation of microwave heating, the depth of penetration (D_p) can be used both to predict how much an object is heated and if it will suffer from cold spots. D_p is the length that a wave will propagate into a surface before its amplitude has been reduced by a factor e^{-1}. The wavelength (λ) in different materials is essential in order to understand basic phenomena inside the microwave oven. Since materials have a variety of conductivities and even some complex electrical parameters the easiest way is to use mathematical definitions in order to calculate wavelength and depth of penetration. Thus the depth and the length should be calculated with equation 2.24 and 2.25, respectively. The complex propagation constant is given by equation 2.26. These complex calculations can be tedious without the use of software that can handle complex values. A solution to that problem is presented in appendix B.

$$D_p = \frac{1}{\mathrm{Re}(\gamma)} \tag{2.24}$$

$$\lambda = \frac{2 \cdot \pi}{\mathrm{Im}(\gamma)} \tag{2.25}$$

$$\gamma = \sqrt{\mathrm{j} \cdot \omega \cdot \mu_r \cdot \mu_0 \cdot (\sigma + \mathrm{j} \cdot \omega \cdot \varepsilon_r \cdot \varepsilon_0)} \tag{2.26}$$

2.9 Ionization in gases

There are many circumstances in which ionization can occur in gases. Air is the gas in question here and the discharge will appear when air changes from an insulator to a conductor. The simplest approach to predict a spark is to use Townsend's breakdown criterion which is stated in equation 2.27 (Cooray 2003b). This criterion suggests that two conductors are placed at a distance d between each other and a constant electric field is applied as well as a constant pressure. The number of ionization collisions made by an electron is denoted α_{ion} (when travelling a unit length) and is given by equation 2.28 where A and B are empirical constants. α_{ion} is often referred to as Townsend's first ionization constant and γ_{ion} is referred to as the second ionization constant. γ_{ion} is the average number of electrons released by each positive ion during secondary ionization.

Different approximations of this can be found in Corray (2003b). This criterion suggests ionization for high values of α_{ion} and γ_{ion} which is related to high electric field (E), low pressure (p) and a significant secondary ionization process.

$$\gamma_{ion} \cdot \left(e^{\alpha_{ion} \cdot d} - 1\right) \geq 1 \tag{2.27}$$

$$\alpha_{ion} = A \cdot p \cdot e^{-\frac{B \cdot p}{E}} \tag{2.28}$$

Townsend's breakdown criterion as stated in equation 2.27 has limited use when applied to heating in microwave oven. There are not two distinct conductors inside the oven and in addition the field is alternating. The solution to this problem is to study corona discharges, where the basic criterion can be extended as in equation 2.29 (Cooray 2003b). This new criterion states that ionization might occur in a region around the conductor, up to the distance x_{limit}. x_{limit} is chosen as the maximum distance (x) where the number of ionization collisions α_{ion} is higher then the number of attachment collisions η_{ion} for the electrons. η_{ion} can be calculated with equation 2.30 (Corray 2003b), where C and D are empirical constants. Comparing equation 2.28 and 2.30 suggests that a high field and a low pressure over a long distance will increase the integral part of equation 2.29. High value of the integration in combination with a high value of the secondary ionization process will result in a breakdown.

$$\gamma_{ion} \cdot \left(e^{\left(\int_0^{x_{limit}} (\alpha_{ion} - \eta_{ion}) dx \right)} - 1 \right) \geq 1 \tag{2.29}$$

$$\eta_{ion} = \frac{C \cdot p^2}{E} \cdot e^{-\frac{D \cdot p}{E}} \tag{2.30}$$

Equation 2.29 states a breakdown criterion that does not require a uniform field and two distinct conductors at fixed distance. The next step would be to introduce fields that vary in time. As long as the breakdown criterion is fulfilled ionization can take place. Even if it is fulfilled only for a short time period ionization can start and result in a spark. Instead of treating the field as periodic in time it can be treated as multiple impulses. One requirement for breakdown is that a free electron is present which is able to start an avalanche. At this instant the field must have a strength above a critical level and remain high enough until the discharge is complete. A time lag can be defined which expresses the time needed from the start of ionization with a free electron to the final breakdown (Corray 2003b). This is a simplification of the problem since the shape of the impulse is not taken into consideration. Free electrons can be created by cosmic radiation or radioactivity in the ground. Since the creation of electrons is random a statistical nature is added to the problem.

The next step would be to use statistical methods to define peak values of the electric field that leads to a certain probability that an impulse would result in breakdown. Defining these values is not a part of this thesis since it would require a vast amount of measurements and mathematical methods.

3 Test method

3.1 Experimental approach to the problem

The problem with the carton is that ionization occurs at the top perforation and in the folding at the bottom of the carton. The sparks only appear at the top when the carton has been ripped open using the perforation. At the bottom the problem occurs when it is folded and jointed. Hence it can be viewed as two different problems that can be solved separately. During the investigation of the problem at the bottom, the top should be cut open with scissors. In the same manner the problem at the top should be studied when the carton has been unfolded and cut open at the bottom, if no other way to prevent ionization is possible. When needed, the bottom can be enclosed with tape to prevent leakage of food.

3.1.1 Top perforated edge problems

In order to make it easy to open the carton there is a perforation around the top. When the top is ripped off, the perforation causes an unevenness of loose paper fibres and a spiky metal foil. When the carton is exposed to microwaves, ionization appears as sparks at the perforation. The sparks are unwanted by the consumer and must be prevented.

3.1.2 The bottom fold edge problem

The bottom consists of many layers, folded close together. Due to the number of layers and the low airflow, the metal foil can be severely heated when the carton is used in a microwave oven. The folding closely resembles a microstrip antenna and has sharp edges. Ionization seems to always occur at the same spots. These discharges can leave marks at the bottom of the oven and even set fire to the paper in the bottom folding. Any such discharge is unwanted for a commercial product.

3.1.3 Cause

There is reason to believe that several factors contribute to ionization. Some of the following properties can be found with literature studies, while others were found by discussions. All of the following properties should be considered during tests:

- Temperature of the metal foil and the air
- Position of the carton in the oven
- Direction of the electric field
- Sharp edges and corners
- Surface currents in the metal foil
- Length of parts of the carton which are close to the resonance length
- Distance between the metal layers
- The field strength inside the microwave oven

- Material properties of the carton

A test case can be chosen in order to investigate the cause of ionization or in order to prevent ionization. It is natural to start with investigating the cause and later, using those results, finding a solution that prevents the problem. If a test case only changes one of the properties it can be used to conclude if that property causes ionization or not. The optimal design is a carton that limits all the properties that contribute to ionization. Due to a large number of possible test cases only the most interesting are covered in this thesis. Those test cases are presented in chapter 3.2.

3.2 Test cases

To understand the phenomena that cause the ionization in the bottom fold edge experimental tests were performed. In the tests a 900 W microwave oven of the brand Whirlpool was used, which is a standard domestic microwave oven. There are some serious problems when electric instruments are used inside a microwave oven, because most cables work as an antenna for microwaves. Therefore our own senses are the only possible way to check when ionization has occurred.

The following part of this chapter lists some important test cases that have been performed. All test cases, except for ordinary cartons with ripped top, have been opened just below the perforation with scissors. With this approach the problem has been isolated to the bottom folding.

3.2.1 Ordinary carton with ripped top

This is the carton as it is today with a laminated foil containing paper, plastic and a thin layer of aluminium. It contains 400 ml and is folded in a way at the bottom which creates two triangles on the outside of the package, which can be seen in figure 3.1.The carton is ripped along the perforated line, the same way as in the instructions printed on the carton.

There are two problems that occur on most *Ordinary carton with ripped top* when they are exposed to microwaves. The most severe ones are the bottom fold edge ionization explained in chapter 3.1.2, and the notable but not crucial top edge ionizations explained in chapter 3.1.1.

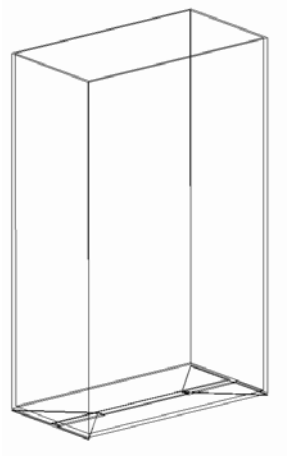

Figure 3.1. This picture illustrates an ordinary carton.

3.2.2 Ordinary carton cut open

This is the carton as mentioned in chapter 3.2.1, with the exception that the carton is cut open at the top with scissors. The folding is shown in figure 3.1.

The ionization at the top is here avoided with a clean cut with scissors. Ripping the carton open would result in an uneven metal edge.

3.2.3 Bottom triangles folded up on the side

Instead of folding the triangles under the package they are folded up on the side of the carton. This can be seen in figure 3.2.

One way to change the form of the bottom fold is to use the same folding technique Tetra Pak uses to seal the top. This folding changes the look of the package in a way that makes it look more symmetric, with the same folding both at the top and the bottom.

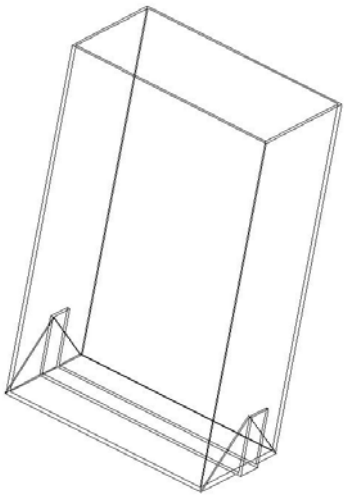

Figure 3.2. This picture illustrates an ordinary carton with the bottom triangles folded up on the side.

3.2.4 Bottom triangles folded out on the side

Instead of folding the triangles underneath the package they are here folded out along the bottom. This folding is illustrated in figure 3.3.

With this change the goal is to see if the results are the same as the test case with triangles folded up on the side or with standard fold with triangles at the bottom. This folding is not a preferable way to make a carton, but it can give information about the nature of the problem.

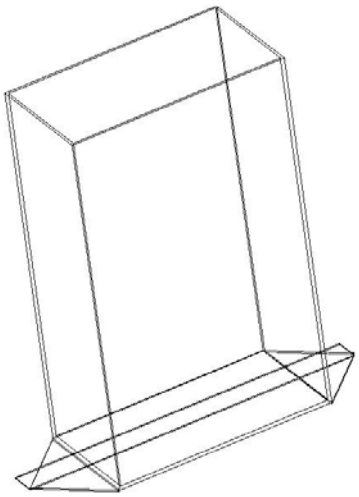

Figure 3.3. This picture illustrates an ordinary carton with the bottom triangles folded out on the side.

3.2.5 Bottom folded out

In this test case the bottom is folded out and the seam is pointing down as can be seen in figure 3.4. The carton has to be balanced in some way, when it is heated in upright position.

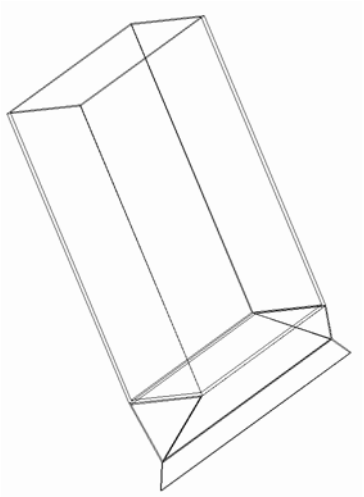

Figure 3.4. This picture illustrates an ordinary carton with the bottom folded out.

3.2.6 Carton opened and laid on the side

Here an ordinary 400 ml carton lying on the side, as viewed in figure 3.5, is considered. The top is closed with adhesive tape in order to enclose the water.

With the carton placed on the side the direction of the electric field is altered in relation to the carton. The carton is tested laying on both of the broadsides.

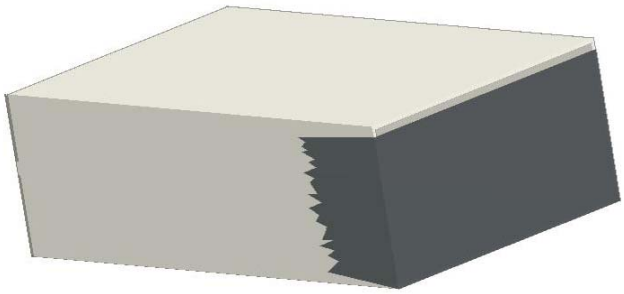

Figure 3.5. This picture illustrates an ordinary carton that is laid on the side. Adhesive tape has been used to prevent leakage of food.

3.2.7 Bottom fold edge altered

The seam in the bottom is normally about 10 mm wide. The seam can be shortened without leaking any fluid. It is also relevant to test the carton when the fold is short-circuited. The bottom fold edge can be joined in different ways. Figure 3.6 shows the fold edge between and below the two triangles.

The bottom seam is the most critical part of the carton when it comes to ionization. It has some similarities to a transmission line and is therefore sensitive for small changes.

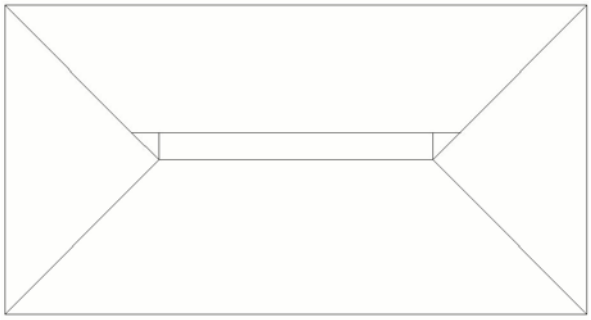

Figure 3.6. This picture shows the way the bottom is folded on an ordinary carton.

3.2.8 Resized carton

The ordinary carton can be resized to some extent. For this test case the same kind of folding in the bottom is used, but the folding and the carton is made smaller.

The resized carton was tested to see if there were any differences in result between this and the larger 400 ml carton. The wave phenomenon is likely to change when the carton is resized.

3.2.9 Carton with cups of water

A standard carton filled with water can be heated with additional water added inside the microwave oven. The extra water is added as a varying amount of cups with a fixed amount of water.

This test was performed in order to see how important the field strength was in the ionization process. The extra water absorbs fields and lowers the average field strength.

3.2.10 Parts of a carton

The carton can be cut into many parts. This test case concerns parts heated individually inside the microwave oven.

If the carton does not behave as an antenna each part of the carton can be tested separately. If the parts are cut out with scissors the new edges are not unnecessary sharp.

3.2.11 Slices in carton

Cuts can be made in the carton with a knife or scissors. Either the cuts should be made thin enough or adhesive tape should be used to prevent leakage.

Cutting out parts of the metal can prevent surface currents. The conductivity of fluids inside the carton should be taken into consideration, since it might short-circuit the slices.

3.3 Temperature measurements

3.3.1 General

Heat can be transferred with conduction, convection and radiation. In addition conduction and radiation can be used to measure temperature (Grahm 1996). Conduction is used when a transducer is placed in contact with the measurement object. Since all objects emit heat radiation a transducer that absorbs radiation is an alternative.

3.3.2 Temperature of interest

One possible reason for the ionization is that the magnetic field induces currents in the metal foil. The current heats the metal foil and the temperature contributes to possible ionization. This temperature can be computed in a simulation, calculated analytically or measured. SEMCAD is not suited to compute the temperature, and to create a new model in a different program is time consuming. The analytical calculations require several approximations and are treated in appendix C.

Unless the sources in SEMCAD are chosen with great care the results will only be presented with relative field strength. However SEMCAD has a feature that calculates specific absorption ratio (*SAR*) in W/kg for arbitrary volumes. The temperature change of water, which is heated for a specific time, can be used to calculate the power that the water is heated with. A comparison between these two power values gives a normalisation value that can be used in SEMCAD to display absolute field strength. Equation 3.1-3.3 can be used for these calculations.

$$P_{\text{Real heating}} = \frac{\Delta T \cdot k \cdot m}{t} \tag{3.1}$$

$$P_{\text{Default scale}} = \frac{SAR}{m} \tag{3.2}$$

$$k_{\text{normalization}} = \frac{P_{\text{Default scale}}}{P_{\text{Real heating}}} \tag{3.3}$$

3.3.3 Choice of method

Not all methods are suitable for temperature measurement inside a microwave oven. If the transducer is placed inside the oven it will be exposed to electromagnetic fields. The field can heat both the transducer and any wires connecting it, resulting in faulty values. In some extreme cases the transducer will break and the wires melt or spark. If wires are connecting between the inside and the outside of the oven they work as an antenna and both conduct and radiate microwaves. That would mainly be hazardous for connected electronics but also for sensitive equipment in the room.

There is an easy way to avoid all the problems connected to temperature measurement during microwave heating. It is to simply purchase a microwave oven with a built in digital temperature measurement suited for heating of food. Then the problems have already been taken care of by the designer. Another way is more expensive but will allow more precise and versatile measurement. If heat radiation is used there is no need for metal conductors and or electronics inside the microwave oven. An infrared camera can give an overall view of the heating process. Infrared diodes can provide point measurements in combination with a digital interface. The metal grating and the glass might affect the result if the beam is forced to cross the window. A good choice is to use equipment with a thin fibre than can be penetrate the oven through a small hole.

The problem with the aluminium foil is its small mass and that it is covered with plastic foil. This can be a problem when trying to measure the temperature even outside the microwave oven. Since the mass of the aluminium is limited any contact probe has to be even smaller, to prevent the transducer and wiring from cooling of the foil. The natural alternative is a touch-free measurement. In both cases it is important to remember that the temperature of the aluminium should be measured and not the temperature of the plastic.

The use of temperature indicating crayons is a cheap and effective method. Although limited to measuring only the peak temperature with a low precision, there are several advantages. The crayons do not seem to be affected by microwaves and can be used to measure temperature in very specific points without cooling of the measuring object. It also requires a minimum effort to apply crayons to specific points.

4 Computations in SEMCAD

This part should not be considered as a manual for simulations in SEMCAD, since there are some critical parts of the simulation process that are not described here. The parts that are not included here are better read in the SEMCAD Reference Manual (http://www.semcad.com/downloads_free/SEMCAD_RefManual.pdf).

4.1 Learn the program

Without any knowledge of SEMCAD it takes some time to get to know the program and all the different features. A good start is to use the SEMCAD-light version which is much cheaper than the full version, however it has some limitations. The light version is not able to create a grid larger than 1 million cells and it is not possible to work with more than 10 volumes. Despite these limitations it is possible to do some tutorials and preparations for the real work by running simplified simulations of the real problem.

4.2 Model design

SEMCAD is a three-dimensional program which gives the possibility to model objects very accurately. The carton is difficult to model perfectly because of the soft materials it is made of and the fact that SEMCAD has problem with curved lines and volumes. This problem is based on that the FDTD method only uses cubic cells and that a lot of cubic elements are required to resemble curved edges.

More and smaller cells give better resolution, but on the other hand it results in more simulation time. It is not only the number of elements that are important for the simulation time but also the size of the smallest cell, which decides what time step that will be used according to equation 2.21. If cells small enough to split every layer of the carton would be applied the simulations would take several weeks, mainly because of the small time step. The solution is to choose an element small enough to resemble the space between the thinnest layers or choose good resolution in just one dimension.

There are three different types of sources which are called plane wave excitation sources, edge sources and wave port excitation sources. Different kinds of sensors can be used dependent on the sort of results that shall be recorded. Both the sources and sensors are placed in the model, even though they are not used to alter any physical characteristics.

4.3 Simulations

When the entire model has been designed, the next step is to switch the program to simulation mode. In simulation mode it is possible to select between two types of simulations, transient and harmonic mode. The transient mode can generate a Gaussian pulse, which is a pulse with a waveform described by the Gaussian distribution. With this kind of sources the simulation has reached a stable condition when all signs of the pulse

have disappeared. In harmonic mode the sources generate a continuous sinusoidal signal that has to reach a steady state for the simulation to be complete. It is harder to get a harmonic simulation to converge.

4.4 Evaluation and post processing

Post-processing is the part that takes place after a simulation is complete. In the post-process menu there are several options on how the results from the simulations can be shown. For example the calculated electric field can be represented by arrows or a colour scale, when viewed in a plane. The fields can even be animated for a time period. The sensors are accessible in a tree structure in a program menu. Each sensor contains different quantities and the results from the completed simulation can be visualized with diagrams. To determine the convergence of the simulations at least one voltage sensor should be placed in the model. One choice is to have one sensor aligned with each axis. Dependent on the type of simulation that is performed the voltage at these sensors should either take form of a sinusoidal signal with constant amplitude or fade out.

One of the most important factors in the ionization process is the magnitude of the electric field. The electric field can be plotted in SEMCAD over the entire sensor volume, which gives information on where critical points and areas are. With a mesh containing small cells it is easier to find spots with high fields, due to the increased resolution.

The result is by default normalized to 1 W input power. Normalization gives the possibility to compare the results to reality. If the default value is used any comparison will be strictly relative, which means it is only possible to see if one carton design is better than another. With knowledge of the actual input power it is possible to make SEMCAD calculate the absolute values of the fields. Calculation of this normalization is treated in chapter 3.3.2.

4.5 Method for using SEMCAD

It is natural to strive for simulations in SEMCAD that are as realistic as possible, which in this case would require an entire microwave oven and the use of harmonic waves. To limit the simulation area it is better to only model the carton, hovering above a small metallic bottom wall. Transient simulations converge easier than harmonic simulations and for this reason transient simulations should be chosen.

A good way to model the waves that would have been generated by the magnetron is to use plane waves. If only one plane wave source was used, the result would be very dependent on the angle and polarization of the incident wave. It is not reasonable to model the complex wave propagation structure inside the oven including reflections from walls and possibly a rotating plate. Instead the best choice is to use many waves with random incident angles and polarizations. If the number of sources is increased from six to twelve the results vary very little between the simulations.

In order to verify the results for long simulations a quick simulation can be performed. Quick simulations can also be used to find any fundamental error in the model or simulation parameters.

As discussed in chapter 2.5 there is a limit on the maximum size of cells, dependent on the wavelength in the material. The wavelength is short in dielectrics such as water requiring high resolution of any food in the model. The simulation time can be reduced when simulations are made without food in the carton.

5 Result

5.1 Simulation result

The simulation results are an important part in the struggle to find a valid explanation to what causes the ionization, especially in the bottom fold. The focus is on the electric field which has been studied in detail after simulations.

5.1.1 Ordinary carton

The cases presented in figure 5.1-5.3 are taken from SEMCAD and illustrates the electric field in different planes. Each figure represents a thin slice of the field at a specific height. The values shown in the figures are absolute and normalized according to chapter 3.3.2. The maximum field strength is found at the bottom corners of the carton.

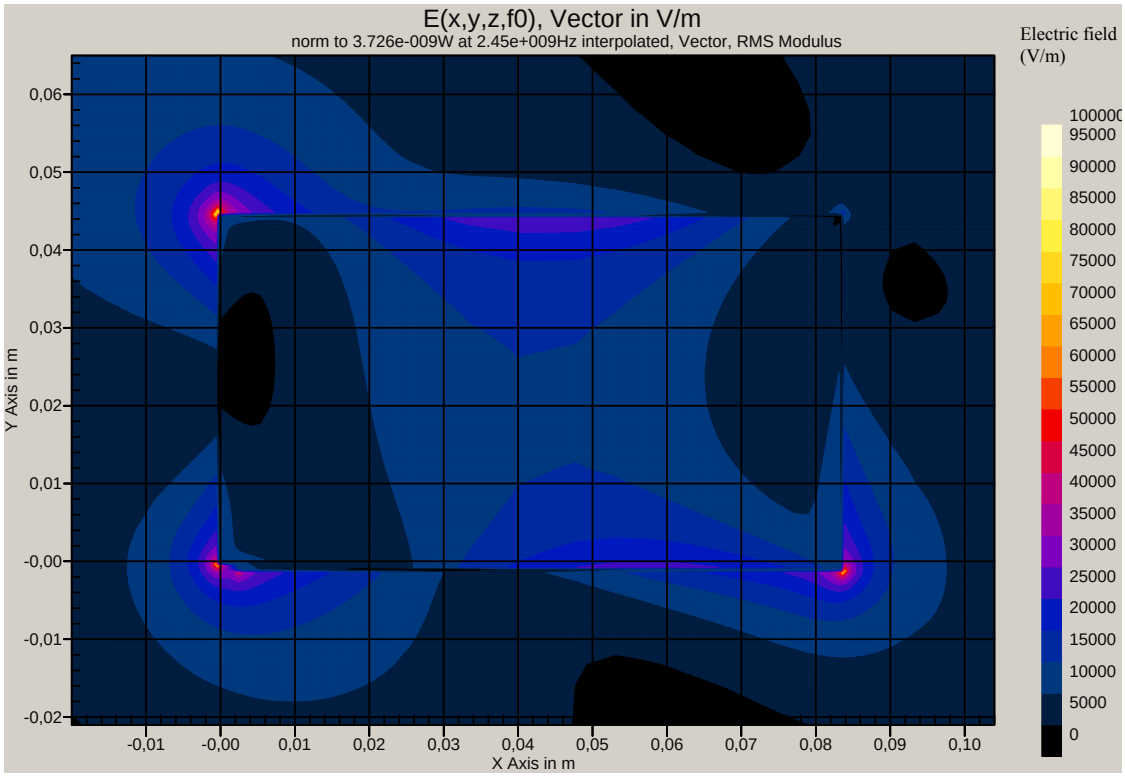

Figure 5.1. Picture in the x-y-plane at the height of the top corners. High electric fields can be seen as bright yellow areas at some of the corners.

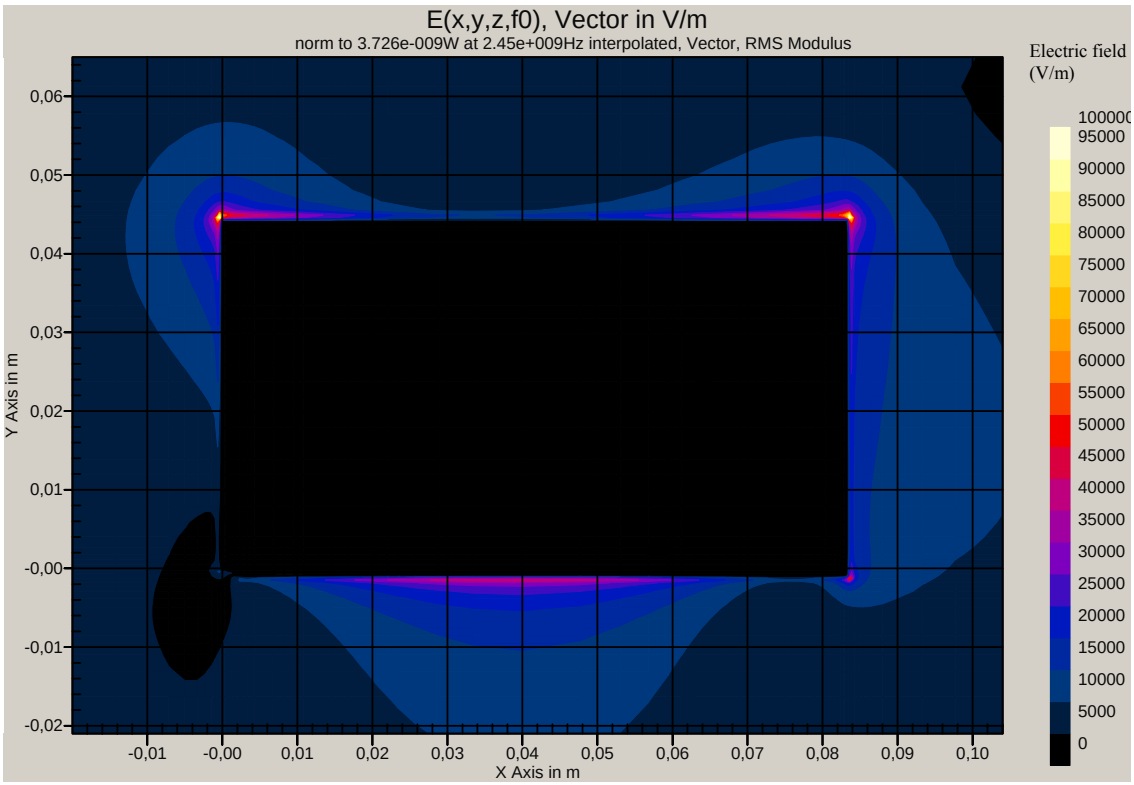

Figure 5.2. Picture in the x-y-plane at the height of the bottom corners. High electric fields can be seen at two of the corners as yellow dots.

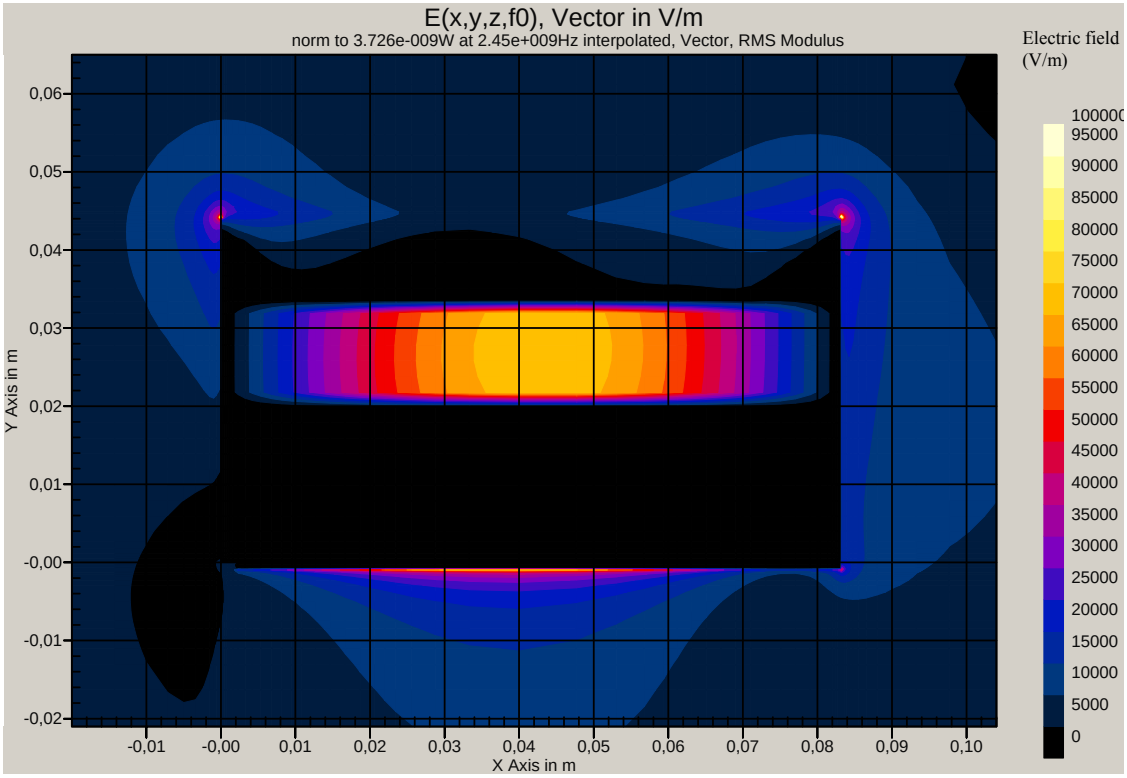

Figure 5.3. Picture in the x-y-plane that shows a standing wave between the metal layers inside the bottom seam. High electric fields can be seen in the seam as a standing wave pattern and in the corners as dots.

5.2 Experimental result

5.2.1 Temperature tests

The temperature indicating crayons showed that the metal foil got heated up to almost 100 °C at most areas, when heated with microwaves. There were some small areas that were heated above 200 °C, these areas where all close to the metal edges.

The increase of temperature in the water during heating in the microwave oven was measured. The ordinary carton was heated with approximately 3 °C per minute. That means that the ordinary carton would require approximately 12 minutes, when heated from room temperature to 60 °C.

5.2.2 Ionization tests

In order to verify the SEMCAD-simulations and finding a solution to the problem experimental tests were performed with real cartons in a microwave oven. The results from the test cases mentioned in chapter 3.2 are listed here in the same order

According to tests the position of the carton inside the microwave oven can not be used to prevent ionization. However any carton might discharge against the oven walls if it is placed too close to any of them. The exact distance is hard to tell, since it is so small that the carton almost touches the wall.

Ordinary carton with ripped top
On almost every package of the ordinary carton, ionization occurs in the bottom fold and at the perforated top. The ionization in the bottom fold is severe and can causes loud flashes and burnt paper. In most cases it appears on both triangles, a burn mark from this kind of ionization can be seen in figure D.1. At the perforation the ionization is more discrete and sometimes difficult to see, but it is possible to hear and observe visually as burnt paper fibres.

Ordinary carton cut open
The ionization problems at the top disappear for the ordinary carton when it is cut open with scissors. However the problem in the bottom folding is not solved.

Bottom triangles folded up on the side
Folding the triangles up on the side is a concept that solves the problem in the bottom fold. Hence there is no ionization when this carton is cut open.

Bottom triangles folded out on the side
For the test case with bottom triangles folded out on the side, ionization still occurs. Burn marks appear at the same places on the triangles as on the ordinary carton.

The bottom folded out
The ionization that occurred when the bottom is folded out was distinct. During ionization some of these cartons even made marks on the inside of the oven.

Carton opened and laid on side
A carton opened and laid on side solves the bottom fold problem with no other changes except positioning, compared to the ordinary carton. This is not a realistic way to solve the problem but it is possible to draw some interesting conclusions.

Bottom fold edge altered
The test case with bottom fold edge altered allows many approaches. Cutting of a thin part of the edge with scissors often prevents ionization, but does not give reliable results. Pinning the edge together with heat limits the ionization problems, but only if the pressure is even. This technique is a bit unreliable.

Resized carton
This carton is much smaller than the standard carton, but it shows the same behaviour as the 400 ml carton in all kind of manners. The same ionization problems appear in the bottom fold and at the top perforation.

Carton with cups of water
By adding and removing cups of water during heating the overall field strength can be altered to some extent. An ordinary carton heated together with cups of water clearly showed that the field strength can be lowered to a point where ionization does not occur. With three cups of water the field strength has been lowered enough to prevent the ionization in the bottom fold. With two cups the ionization starts again. The power distributed into the cavity is probably a very important factor in this test case.

Parts of a carton
Heating individual parts of a carton inside the oven gives random and unpredictable results dependent on geometry of the cut out object. If part of the folding is heated it might not cause ionization as in the case with the entire carton. In addition, parts of the carton that usually are trouble free can give problems. Curved shapes give overall better ionization immunity.

Slices in carton
As a test case slices can be cut in many ways. Cutting out parts of the metal generally only creates problems at the new edges. The results when cutting out parts of the carton seem random and unpredictable.

6 Discussion

6.1 Discussion of simulations

6.1.1 Discussion of simulation methods

It is not possible to model the carton inside a complete microwave oven in SEMCAD, with reasonable accuracy and computation time. Even when modelling only a carton without microwave oven the simulations take too long time to allow optimization tests. The major reason for long simulation time is the limit on time step, as seen in equation 2.21. In order to resolve small details in the folding the time step gets short, resulting in too many simulation steps. If the resolution is chosen too low only averages of small areas are available rather than the value of the fields in specific points.

One way to avoid the problem with simulation time is to use many computers and running multiple simulations at once. A small program called SEMLAB can be used to run simulations without graphical interface on almost any kind of computer. The idea would be to prepare all simulations on a single computer using SEMCAD and to run simulations on other computers with SEMLAB. Unfortunately this was not an option in this project, since the number of computers was limited and SEMLAB was not part of the license package available.

In this project the most important application of SEMCAD is for comprehension. In an early stage of optimization SEMCAD can be used to find critical points where fields accumulate. A few simulations in SEMCAD can give an understanding of wave phenomena and field accumulation, which is of great use during experimental optimization. In addition, due to limited measuring equipment SEMCAD is needed in order to find a value of the fields inside a microwave oven.

The usage of SEMCAD was chosen early in this project since the original problem description suggested a comparison between software simulation and experimental tests. However it turned out that the software did not have the major role during optimization. In either case it has been very educational to learn using SEMCAD and studying the simulation results.

Simulations based on the same model with different resolution give almost the same results. The only noticeable difference is the resolution of the result.

The number of cells needed during simulation can be reduced by not including any food in the model. Results from most of these simulations vary little compared to ordinary simulations.

Several simulations have been run with different sources with random angles of incidence. In the results from these simulations, the critical points are the same but the mutual values of the field strength vary between the corners. The variation of field

strength at the critical point is probably dependent on where the sources amplify and attenuate each other.

6.1.2 Discussion of simulation results

As seen in some figures, for example figure 5.1, the fields generally accumulate at sharp corners. The figures can be a bit conceiving since the carton corners are modelled much sharper than they are in reality. The corners are modelled sharp since the grid in SEMCAD is based on cubes. The field strength at some critical points is comparable to the breakdown potential of air, which is approximately $3 \cdot 10^6$ V/m (Cooray 2003a). When a small amount of cells are used the resolution is limited. The maximum fields at critical points will show lower values when the resolution is low, since an average value is displayed instead of the value at a specific point. In figure 5.3 a standing wave can be clearly seen, which is most likely caused by a transmission line effect. There is also reason to believe that the folding at the bottom of the carton can work as a folded microstrip antenna. Combining these two effects can explain the critical field accumulation at the folding edges.

The frequency of microwaves generated by a magnetron can differ slightly. To investigate if this will affect ionization a simulation can be run with multiple frequencies. Simulations at neighbouring frequencies give almost identical results and have been left out of this report.

6.2 Discussion of experimental tests

6.2.1 Discussion of temperature method

The problems concerning temperature measurements have been treated in chapter 3.3.3. Measurements inside the microwave oven have been made with temperature indicating crayons. These crayons were first tested against an independent touch-free thermometer during the heating of a frying pan. The crayons proved to be accurate in temperature and both legible and quick in change of colour. Some simple tests inside the oven indicate that microwaves will not effect the chemical reactions in any harmful way.

The measurement of the food temperature does not need to be made in a complicated way. Simply taking the carton out of the oven, stirring and adding a thermometer proved to be accurate enough. The simplicity of conductive thermometers leaves few sources of error. Cooling of the food against air can be negligible due to the short time it takes to make a measurement. The thermometer will cool the food, but this effect is limited due to the size of the thermometer relative to the food.

6.2.2 Discussion of temperature results

The measured temperatures seem reasonable and comply to some extent with calculations made in appendix C. Since high temperatures only were measured at edges the heating is likely to be caused by accumulation of fields.

Since a typical microwave oven is supplied with the power 900 W the magnetron generates microwaves with heating capacity of the same order. The magnetron generates waves independent of what is inside the oven. This leads to a surplus of power when a standard carton with a lot of shielding aluminium foil is used relative a non shielded amount of water. This power will to some extent be reflected back to the magnetron and reduce its lifetime (Vollmer 2004).

6.2.3 Discussion of ionization tests

All ionization tests were performed in the same microwave oven. Using the same oven is useful when comparing different cartons and makes it easier to draw conclusions. A disadvantage is that the final results can not be generalized to the same extent, but since most microwave ovens are similar this is a minor problem. In order to confirm the validity of each test case the function of the oven was verified between every test. An easy way to verify the oven is to check the time it takes to heat a specific amount of water to a specific temperature.

As already mentioned, only the most interesting test cases are covered in this report. All test cases mentioned have been tested several times both with and without small changes. The number of tests and the small changes made between the tests are not covered due to the vast amount of data that would have to be listed and explained. Due to the limited data listed some results, suggestions and conclusions might seem a bit far fetched.

The test cases have been chosen to draw conclusions of the properties mentioned in chapter 3.1.3. The only property that has not been fully considered is the material property. Only limited variations of material properties have been available and it was not enough to draw any conclusions.

Moving a carton around can be used to test if the positioning can prevent ionization. This has not been treated as a specific test case.

6.2.4 Discussion of ionization results

Discharges between the carton and the walls in the microwave oven only occur when the distance is small. The walls inside the oven are connected to the same ground that is used for the supply voltage of the oven, which might encourage this kind of discharges. This kind of discharge has not been examined in this thesis since it is natural to place the carton in the centre of the oven during heating.

As can be seen in SEMCAD, fields tend to accumulate at sharp corners and edges. When the carton is ripped open small edges are created by the perforation compared to when it is cut open by scissors. Such edges are too small and random to be simulated in SEMCAD. A comparison between the cases when the ordinary carton is opened with and without perforation, suggests that the accumulation of fields is the cause of ionization at the top of the carton.

Unfolding the edges as in *Bottom triangles folded out on the side* might increase the edge problems. On the other hand the other properties are changed as well. In this case the edge problems seem to be the dominant factor since ionization occurs at the edge of the triangles as in the test case *ordinary carton cut open*.

When the test case *Bottom triangles folded out on the side* is heated in the microwave oven there is still a problem with ionization. When the folding is made this way the temperature at the edges is reduced due to better circulation of air, in addition the possibility of discharge between metal layers at the bottom is limited. Since ionization still occurs it is likely that temperature and distance between layers can not be used to prevent ionization. Unfolding the carton in a different way results in a new test case called *bottom folded out*. Similarly this test case also has problems with ionization. This test case has good air circulation and limited amount of adjacent metal layers but has a different direction of the folding edge compared to the fields. Even if the temperature and distance between layers are irrelevant the change of field direction does not seem to be enough to prevent ionization for this test case.

The only significant difference between *Resized carton* and the ordinary carton is the size. Since the test results are completely similar for these two cases it is suggested that the length of individual parts is unrelated to ionization.

The major difference between *Carton opened and laid on the side* and the standard carton is the direction of the field components at the folding. This test case is a solution to the ionization problem, but it is not suitable as a commercial product for several reasons. This test clearly shows that the direction of the field components is a relevant property.

Bottom triangles folded up on the side is one possible solution to the ionization problem. The major difference between this test case and the ordinary carton is the direction of the electric field in relation to the cartons triangle edges. Comparing to *Bottom triangles folded out on the side* this effect alone seems to be enough to prevent ionization.

The bottom fold edge can be altered in many ways that prevent ionization. The current machine process results in an edge that has small bends and is shaped like a horn antenna at the opening. Whether the edge is short-circuited or not varies between the manufactured cartons. The techniques used in *Bottom fold edge altered* were never perfected or compared to possible solutions for mass production. It seems like alteration of the bottom edge can be a simple and effective solution to the ionization problem at the bottom.

The two test cases *Parts of carton* and *Slices in carton* show that the different parts of the carton can not be treated individually. The carton can be compared to an antenna where surface currents play a distinctive role. It is hard to repeat experimental tests concerning surface currents and receiving the same result. Optimizations of this kind should preferably be made with software simulations. From the experimental tests that have been performed, it is clear that changes that alter surface currents can affect ionization. Those

kinds of changes generally give only new problems rather than solving the initial problem, when optimization is made with experimental tests.

6.3 Comparison of simulation result and experimental result

Since the field strength given by SEMCAD is close to the breakdown voltage it is likely that ionization will occur for the ordinary carton. This complies with the experimental results where ionization in fact does occur. The spots with critical fields in SEMCAD do not agree with where ionization does occur in experimental tests. This is probably only related to limits in the SEMCAD-model.

Spots and edges with high field strength can easily be found in SEMCAD and it is natural that the magnetic field induces surface currents that heat the metal. The spots and edges with high fields found in SEMCAD also have higher temperature in experimental tests.

When food with bad circulation is heated in an oven cold and hot spots can be found. These hot and cold spots can be found in SEMCAD as parts of the food with more or less heating fields.

7 Conclusion

There are many factors, especially manufacturing aspects, to take into consideration. This complicates the possibility to present a complete solution. The listed conclusions will not solve the problem completely for Tetra Recart, it should rather be used as a ground for further work.

7.1 Conclusion from simulations

It is difficult to use SEMCAD as an optimization tool when simulating a thin metal carton. This is mainly because of the long simulation time, due to the fine resolution required in this thesis.

Electric fields accumulate at sharp metal edges. SEMCAD is able to give an absolute value of the field strength in a microwave oven if a normalization method is used as in chapter 3.3.2.

It is evident that the simulation results do not match the reality perfectly. The most obvious factor that affects the results is the differences between the three-dimensional model made in the computer and the real carton. The cell approximation in SEMCAD is an important factor contributing to a result that differs from reality.

7.2 Conclusion from experimental tests

Ionization in the bottom fold can be avoided with a different folding or with a different manufacturing method of the bottom seam, see chapter 6.2.4. The direction of the electric field is also important for the ionization process in the bottom fold. Ionization is strongly related to sharp edges and high electric fields, as described in chapter 2.9. This is important both in the top perforation problem as well as in the bottom fold problem.

There are two possible solutions based on an *Ordinary carton cut open* and one that is attractive in a manufacturing aspect. A carton with the bottom fold triangles fold up on the side will solve the ionization problem and it is a solution that is possible for manufacturing. If the carton is laid on the side there is no ionization problem, though it is not a good solution for the users.

High temperature can be measured at specific points when the aluminium foil in the carton is exposed to microwaves. The metal is heated at edges by accumulation of fields and the problem with ionization cannot be prevented by reducing the temperature. Neither can the size of the carton be used to prevent ionization.

7.3 Further work

The perforation at the top edge of an open carton is not suitable for use in microwave ovens unless the fragments of aluminium foil or their electric behaviour is altered. It is difficult to avoid ionization when there is a perforation with small sharp edges. This is an area where more work has to be done, either to find a new solution or to alter the existing perforation. Altering the bottom fold has shown good results and is a promising way to solve the problem in the bottom fold and should therefore be further evaluated.

The time it takes to heat the food in an ordinary carton is too long and might damage the microwave oven. There should be more investigation on how the oven is affected before it is presented as a commercial product, with the recommendation to use it in a microwave oven.

References

Bondeson, Anders - Rylandes, Thomas - Ingelström, Pär (2002). *COMPUTATIONAL ELECTROMAGNETICS*, School of Electrical and Computer Engineering, Göteborg.

Cheng, David K (1983). *FIELD AND WAVE ELECTRORMAGNETICS*, Addison-Wesley Publishing Company, Inc.

Cooray, Vernon (2003a). *Blixten Så fungerar naturens fyrverkeri*, Uppsala Universitet, Uppsala.

Cooray, Vernon (2003b) *The Lightning Flash*, MPG Books Limited, Bodmin.

Grahm, Lennart - Jubrink, Hans-Gunnar - Lauber, Alexander (1996). *Modern industriell mätteknik*, KFS AB, Lund.

Karlsson, Anders - Kristensen, Gerhard (1996). *Mikrovågsteori*, Lunds Tekniska Högskola, Lund.

Risman, Per O - Cleuch-Marcysiak, Malgorzata (2000). ELECTROMAGNETIC MODELLING FOR MIROWAVE HEATING APPLICATIONS, *Microwaves, Radar and Wireless Communications*, vol.3, 167-182.

Roddy, Dennis (1986). *Microwave Technology*, Prentice-Hall, Englewood Cliffs.

Schimid & Partner Engineering AG (2004-12-02), *FEATURES: SOLVERS: FDTD ENHANCEMENTS*, http://www.semcad.com/solver_enhancements.html

Schimid & Partner Engineering AG (2004-12-02), *SEMCAD Reference Manual*, http://www.semcad.com/downloads_free/SEMCAD_RefManual.pdf

Taflove, Allen - Hagness, Susan C (2000). *Computational Electrodynamics: The Finite-Difference Time-Domain Method*, ARTECH HOUSE, Norwood.

Vollmer, Michael - Möllmann, Klaus-Peter - Karstädt, Detlef (2004). Microwave oven experiments with metals and light sources, *Physics Education*, 39 (6), s. 500-508.

Appendix A

Equations for a leap frog algorithm

Equations for a leap frog algorithm based on the Yee space lattice are presented below. Derivation of these equations is made in Taflove (2000), and is presented briefly in chapter 2.4.

$$E_x\Big|_{i,j+\frac{1}{2},k+\frac{1}{2}}^{n+\frac{1}{2}} = \frac{1-\frac{\sigma_{i,j+\frac{1}{2},k+\frac{1}{2}}\cdot\Delta t}{2\cdot\varepsilon_{i,j+\frac{1}{2},k+\frac{1}{2}}}}{1+\frac{\sigma_{i,j+\frac{1}{2},k+\frac{1}{2}}\cdot\Delta t}{2\cdot\varepsilon_{i,j+\frac{1}{2},k+\frac{1}{2}}}}\cdot E_x\Big|_{i,j+\frac{1}{2},k+\frac{1}{2}}^{n-\frac{1}{2}}$$

$$+\frac{\frac{\Delta t}{\varepsilon_{i,j+\frac{1}{2},k+\frac{1}{2}}}}{1+\frac{\sigma_{i,j+\frac{1}{2},k+\frac{1}{2}}\cdot\Delta t}{2\cdot\varepsilon_{i,j+\frac{1}{2},k+\frac{1}{2}}}}\cdot\left(\frac{H_z\Big|_{i,j+1,k+\frac{1}{2}}^{n}-H_z\Big|_{i,j,k+\frac{1}{2}}^{n}}{\Delta y}-\frac{H_y\Big|_{i,j+\frac{1}{2},k+1}^{n}-H_y\Big|_{i,j+\frac{1}{2},k}^{n}}{\Delta z}-J_{source_x}\Big|_{i,j+\frac{1}{2},k+\frac{1}{2}}^{n}\right)$$

$$E_y\Big|_{i-\frac{1}{2},j+1,k+\frac{1}{2}}^{n+\frac{1}{2}} = \frac{1-\frac{\sigma_{i-\frac{1}{2},j+1,k+\frac{1}{2}}\cdot\Delta t}{2\cdot\varepsilon_{i-\frac{1}{2},j+1,k+\frac{1}{2}}}}{1+\frac{\sigma_{i-\frac{1}{2},j+1,k+\frac{1}{2}}\cdot\Delta t}{2\cdot\varepsilon_{i-\frac{1}{2},j+1,k+\frac{1}{2}}}}\cdot E_y\Big|_{i-\frac{1}{2},j+1,k+\frac{1}{2}}^{n-\frac{1}{2}}$$

$$+\frac{\frac{\Delta t}{\varepsilon_{i-\frac{1}{2},j+1,k+\frac{1}{2}}}}{1+\frac{\sigma_{i-\frac{1}{2},j+1,k+\frac{1}{2}}\cdot\Delta t}{2\cdot\varepsilon_{i-\frac{1}{2},j+1,k+\frac{1}{2}}}}\cdot\left(\frac{H_x\Big|_{i-\frac{1}{2},j+1,k+1}^{n}-H_x\Big|_{i-\frac{1}{2},j+1,k}^{n}}{\Delta z}-\frac{H_z\Big|_{i,j+\frac{1}{2},k+\frac{1}{2}}^{n}-H_z\Big|_{i-1,j+\frac{1}{2},k+\frac{1}{2}}^{n}}{\Delta x}-J_{source_y}\Big|_{i-\frac{1}{2},j+1,k+\frac{1}{2}}^{n}\right)$$

$$E_z\left|_{i-\frac{1}{2},j+\frac{1}{2},k+1}^{n+\frac{1}{2}}\right. = \frac{1-\frac{\sigma_{i-\frac{1}{2},j+\frac{1}{2},k+1}\cdot\Delta t}{2\cdot\varepsilon_{i-\frac{1}{2},j+\frac{1}{2},k+1}}}{1+\frac{\sigma_{i-\frac{1}{2},j+\frac{1}{2},k+1}\cdot\Delta t}{2\cdot\varepsilon_{i-\frac{1}{2},j+\frac{1}{2},k+1}}}\cdot E_y\left|_{i-\frac{1}{2},j+\frac{1}{2},k+1}^{n-\frac{1}{2}}\right.$$

$$+\frac{\frac{\Delta t}{\varepsilon_{i-\frac{1}{2},j+\frac{1}{2},k+1}}}{1+\frac{\sigma_{i-\frac{1}{2},j+\frac{1}{2},k+1}\cdot\Delta t}{2\cdot\varepsilon_{i-\frac{1}{2},j+\frac{1}{2},k+1}}}\cdot\left(\frac{H_y\left|_{i,j+\frac{1}{2},k+1}^{n}\right. - H_y\left|_{i-1,j+\frac{1}{2},k+1}^{n}\right.}{\Delta x} - \frac{H_x\left|_{i-\frac{1}{2},j+1,k+1}^{n}\right. - H_x\left|_{i-\frac{1}{2},j,k+1}^{n}\right.}{\Delta y} - J_{source_z}\left|_{i-\frac{1}{2},j+\frac{1}{2},k+1}^{n}\right.\right)$$

$$H_x\left|_{i-\frac{1}{2},j+1,k+1}^{n+1}\right. = \frac{1-\frac{\sigma^*_{i-\frac{1}{2},j+1,k+1}\cdot\Delta t}{2\cdot\mu_{i-\frac{1}{2},j+1,k+1}}}{1+\frac{\sigma^*_{i-\frac{1}{2},j+1,k+1}\cdot\Delta t}{2\cdot\mu_{i-\frac{1}{2},j+1,k+1}}}\cdot H_x\left|_{i-\frac{1}{2},j+1,k+1}^{n}\right.$$

$$+\frac{\frac{\Delta t}{\mu_{i-\frac{1}{2},j+1,k+1}}}{1+\frac{\sigma^*_{i-\frac{1}{2},j+1,k+1}\cdot\Delta t}{2\cdot\mu_{i-\frac{1}{2},j+1,k+1}}}\cdot\left(\frac{E_y\left|_{i-\frac{1}{2},j+1,k+\frac{3}{2}}^{n+\frac{1}{2}}\right. - E_y\left|_{i-\frac{1}{2},j+1,k+\frac{1}{2}}^{n+\frac{1}{2}}\right.}{\Delta z} - \frac{E_z\left|_{i-\frac{1}{2},j+\frac{3}{2},k+1}^{n+\frac{1}{2}}\right. - E_z\left|_{i-\frac{1}{2},j+\frac{1}{2},k+1}^{n+\frac{1}{2}}\right.}{\Delta y} - M_{source_x}\left|_{i-\frac{1}{2},j+1,k+1}^{n+\frac{1}{2}}\right.\right)$$

$$H_y\Big|_{i,j+\frac{1}{2},k+1}^{n+1} = \frac{1-\dfrac{\sigma^*_{i,j+\frac{1}{2},k+1}\cdot\Delta t}{2\cdot\mu_{i,j+\frac{1}{2},k+1}}}{1+\dfrac{\sigma^*_{i,j+\frac{1}{2},k+1}\cdot\Delta t}{2\cdot\mu_{i,j+\frac{1}{2},k+1}}}\cdot H_y\Big|_{i,j+\frac{1}{2},k+1}^{n}$$

$$+\frac{\dfrac{\Delta t}{\mu_{i,j+\frac{1}{2},k+1}}}{1+\dfrac{\sigma^*_{i,j+\frac{1}{2},k+1}\cdot\Delta t}{2\cdot\mu_{i,j+\frac{1}{2},k+1}}}\cdot\left(\frac{E_z\Big|_{i+\frac{1}{2},j+\frac{1}{2},k+1}^{n+\frac{1}{2}} - E_z\Big|_{i-\frac{1}{2},j+\frac{1}{2},k+1}^{n+\frac{1}{2}}}{\Delta x} - \frac{E_x\Big|_{i,j+\frac{1}{2},k+\frac{3}{2}}^{n+\frac{1}{2}} - E_x\Big|_{i,j+\frac{1}{2},k+\frac{1}{2}}^{n+\frac{1}{2}}}{\Delta z} - M_{source_y}\Big|_{i,j+\frac{1}{2},k+1}^{n+\frac{1}{2}}\right)$$

$$H_z\Big|_{i,j+1,k+\frac{1}{2}}^{n+1} = \frac{1-\dfrac{\sigma^*_{i,j+1,k+\frac{1}{2}}\cdot\Delta t}{2\cdot\mu_{i,j+1,k+\frac{1}{2}}}}{1+\dfrac{\sigma^*_{i,j+1,k+\frac{1}{2}}\cdot\Delta t}{2\cdot\mu_{i,j+1,k+\frac{1}{2}}}}\cdot H_z\Big|_{i,j+1,k+\frac{1}{2}}^{n}$$

$$+\frac{\dfrac{\Delta t}{\mu_{i,j+1,k+\frac{1}{2}}}}{1+\dfrac{\sigma^*_{i,j+1,k+\frac{1}{2}}\cdot\Delta t}{2\cdot\mu_{i,j+1,k+\frac{1}{2}}}}\cdot\left(\frac{E_x\Big|_{i,j+\frac{3}{2},k+\frac{1}{2}}^{n+\frac{1}{2}} - E_x\Big|_{i,j+\frac{1}{2},k+\frac{1}{2}}^{n+\frac{1}{2}}}{\Delta y} - \frac{E_y\Big|_{i+\frac{1}{2},j+1,k+\frac{1}{2}}^{n+\frac{1}{2}} - E_y\Big|_{i-\frac{1}{2},j+1,k+\frac{1}{2}}^{n+\frac{1}{2}}}{\Delta x} - M_{source_z}\Big|_{i,j+1,k+\frac{1}{2}}^{n+\frac{1}{2}}\right)$$

Appendix B

Depth of penetration and wavelength

Equation 2.24 and 2.25 are valid for complex values. If no approximation is made, calculations based on these equations are tedious to compute by hand. If no software is available that can handle complex values the following brief derivation is useful. The derivation is based on equation 2.24 and 2.25 which are repeated here as equation B.1 and equation B.2.

$$D_{\mathrm{p}} = \frac{1}{\mathrm{Re}(\gamma)} \tag{B.1}$$

$$\lambda = \frac{2 \cdot \pi}{\mathrm{Im}(\gamma)} \tag{B.2}$$

The equation

$$\gamma = \sqrt{\mathrm{j} \cdot \omega \cdot \mu_{\mathrm{r}} \cdot \mu_0 \cdot (\sigma + \mathrm{j} \cdot \omega \cdot \varepsilon_{\mathrm{r}} \cdot \varepsilon_0)}$$

can be rewritten as

$$\gamma = \sqrt{-\omega^2 \cdot \mu_{\mathrm{r}} \cdot \mu_0 \cdot \varepsilon_{\mathrm{r}}^{'} \cdot \varepsilon_0 + j \cdot \omega \cdot \mu_{\mathrm{r}} \cdot \mu_0 \cdot (\sigma - \omega \cdot \varepsilon_{\mathrm{r}}^{''} \cdot \varepsilon_0)},$$

using the notation

$$\varepsilon_{\mathrm{r}} = \varepsilon_{\mathrm{r}}^{'} + j \cdot \varepsilon_{\mathrm{r}}^{''}.$$

Since this expression for γ now is the root of a real value and an imaginary value the relation

$$(a + jb)^{\frac{1}{2}} = c + jd \Rightarrow$$
$$\begin{cases} c = \sqrt{\frac{a}{2} \pm \frac{1}{2} \cdot \sqrt{a^2 + b^2}} \\ d = \sqrt{-\frac{a}{2} \pm \frac{1}{2} \cdot \sqrt{a^2 + b^2}} \end{cases}$$

can be applied. Using this relation γ can be written with distinct real part and imaginary part as

$$\gamma = \sqrt{\frac{-\omega^2 \cdot \mu_r \cdot \mu_0 \cdot \varepsilon_r^{'} \cdot \varepsilon_0}{2} \pm \frac{1}{2} \cdot \sqrt{\omega^4 \cdot \mu_r^2 \cdot \mu_0^2 \cdot \varepsilon_r^{'2} \cdot \varepsilon_0^2 + \omega^2 \cdot \mu_r^2 \cdot \mu_0^2 \left(\sigma - \omega \cdot \varepsilon_r^{''} \cdot \varepsilon_0\right)^2}}$$
$$+ j \cdot \sqrt{\frac{\omega^2 \cdot \mu_r \cdot \mu_0 \cdot \varepsilon_r^{'} \cdot \varepsilon_0}{2} \pm \frac{1}{2} \cdot \sqrt{\omega^4 \cdot \mu_r^2 \cdot \mu_0^2 \cdot \varepsilon_r^{'} \cdot \varepsilon_0^2 + \omega^2 \cdot \mu_r^2 \cdot \mu_0^2 \cdot \left(\sigma - \omega \cdot \varepsilon_r^{''} \cdot \varepsilon_0\right)^2}}$$

This equation can be used to rewrite equation B.1 equation B.2 using only real valued quantities. That means that D_p and λ can be calculated exactly without software that handles complex numbers, with the equations below.

$$D_p = \frac{1}{\sqrt{\frac{-\omega^2 \cdot \mu_r \cdot \mu_0 \cdot \varepsilon_r^{'} \cdot \varepsilon_0}{2} \pm \frac{1}{2} \cdot \sqrt{\omega^4 \cdot \mu_r^2 \cdot \mu_0^2 \cdot \varepsilon_r^{'2} \cdot \varepsilon_0^2 + \omega^2 \cdot \mu_r^2 \cdot \mu_0^2 \left(\sigma - \omega \cdot \varepsilon_r^{''} \cdot \varepsilon_0\right)^2}}}$$

$$\lambda = \frac{2 \cdot \pi}{\sqrt{\frac{\omega^2 \cdot \mu_r \cdot \mu_0 \cdot \varepsilon_r^{'} \cdot \varepsilon_0}{2} \pm \frac{1}{2} \cdot \sqrt{\omega^4 \cdot \mu_r^2 \cdot \mu_0^2 \cdot \varepsilon_r^{'} \cdot \varepsilon_0^2 + \omega^2 \cdot \mu_r^2 \cdot \mu_0^2 \cdot \left(\sigma - \omega \cdot \varepsilon_r^{''} \cdot \varepsilon_0\right)^2}}}$$

Appendix C

Temperature calculated with the heat equation

Temperature of the metal in the carton can be calculated analytically with the heat equation. The calculations will require a simple structure of layers, some boundary conditions, temperature at boundaries and thermal properties of the materials. A simple structure of layers is presented in figure C.1. The heat equation is stated in equation C.1, where Ξ is the source term.

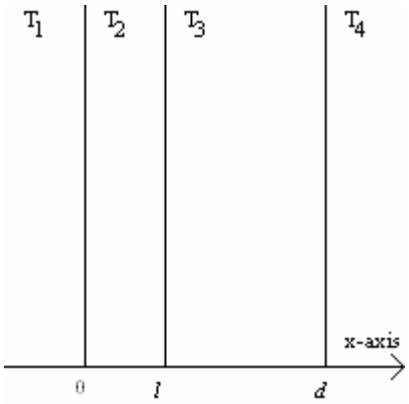

Figure C.1. A structure of layers representing a part of the carton. The figure is divided into four areas. The layers are air, metal, paper and air enumerated from left to right.

$$k_\sigma \cdot \frac{\partial^2}{\partial x^2} T(x) + \Xi(x) = 0 \qquad \text{(C.1)}$$

Due to the depth of penetration in metal compared to paper only the metal is heated directly by microwaves. For simplicity, since the thickness of the metal layer is comparable to the depth of penetration, heating of the metal is considered uniform at all depths. The air around the carton is considered to have good circulation and hence has constant temperature. With these approximations the temperature $T(x)$ in figure C.1 has to satisfy equations C.2. The requirements of equations C.2 gives temperature variation on the form of equations C.3. The temperatures a_1 and a_4 are considered known and the coefficients a_2, a_3, b_2 and b_3 are the only unknowns.

$$\begin{cases} \dfrac{\partial}{\partial x}T(x) = 0, \ x < 0 \\ \dfrac{\partial^2}{\partial x^2}T(x) = -\dfrac{\Xi}{k_{\sigma,2}}, \ 0 < x < l \\ \dfrac{\partial^2}{\partial x^2}T(x) = 0, \ l < x < d \\ \dfrac{\partial}{\partial x}T(x) = 0, \ d < x \end{cases} \tag{C.2}$$

$$\begin{cases} T(x) = a_1, \ x < 0 \\ T(x) = -\dfrac{\Xi}{2k_{\sigma,2}} \cdot x^2 + a_2 \cdot x + b_2, \ 0 < x < l \\ T(x) = a_3 \cdot x + b_3, \ l < x < d \\ T(x) = a_4, \ d < x \end{cases} \tag{C.3}$$

The next step is to introduce boundary conditions. Heat transfer due to convection is not taken into consideration, which limits the heat transfer to conduction and radiation. Conduction occurs between the paper and the metal and forces both the temperature and the first derivative to be constant at the boundary. Since air has limited heat conductivity only radiation is considered at the two remaining boundaries. The heat radiation is dependent on the temperature difference at the boundary and the material properties. The boundary conditions are summarized in equations C.4.

$$\begin{cases} \dfrac{\partial}{\partial x}T_2(0) = \dfrac{\alpha_2}{k_{\sigma,2}} \cdot (T_2(0) - T_1(0)) \\ T_2(l) = T_3(l) \\ k_{\sigma,2} \cdot \dfrac{\partial}{\partial x}T_2(l) = k_{\sigma,3} \cdot \dfrac{\partial}{\partial x}T_3(l) \\ \dfrac{\partial}{\partial x}T_3(d) = -\dfrac{\alpha_3}{k_{\sigma,3}} \cdot (T_3(d) - T_4(d)) \end{cases} \tag{C.4}$$

A system of equations can be created by substituting equations C.3 into equations C.4. The resulting system of equations is written in equations C.5 on matrix form. It is recommended to solve the matrix system with a program such as MATLAB but it can be done by hand. Once the unknowns are calculated the temperature at an arbitrary point is given by equations C.3. The calculations require that the material properties, dimensions of layers and the source are known.

$$\begin{pmatrix} 1 & 0 & -\frac{\alpha_2}{k_{\sigma,2}} & 0 \\ l & -l & 1 & -1 \\ k_{\sigma,2} & -k_{\sigma,3} & 0 & 0 \\ 0 & 1+\frac{\alpha_3 \cdot d}{k_{\sigma,3}} & 0 & \frac{\alpha_3}{k_{\sigma,3}} \end{pmatrix} \cdot \begin{pmatrix} a_2 \\ a_3 \\ b_2 \\ b_3 \end{pmatrix} = \begin{pmatrix} -\frac{a_1 \cdot \alpha_2}{k_{\sigma,2}} \\ \frac{\Xi \cdot l^2}{2k_{\sigma,2}} \\ \Xi \cdot l \\ \frac{a_4 \cdot \alpha_3}{k_{\sigma,3}} \end{pmatrix} \tag{C.5}$$

There are two kinds of material properties involved in the solution of the heat equation. k_σ is the thermal conductivity and can be found for most materials. The emissivity α is rarely stated in literature but can be calculated from the emission factor e. The boundary condition in equation C.6 has been used in equations C.4. This boundary condition is only an approximation based on equation C.7. Equation C.6 is easier to use but is only valid for small variations of temperature.

$$\frac{\partial}{\partial x} T(x) = \frac{\alpha}{k} \cdot (T(x) - T_0(x)) \tag{C.6}$$

$$k \cdot \frac{\partial T(x)}{\partial x} = e \cdot \sigma_B \cdot \left(T^4(x) - T_0^4(x)\right) \tag{C.7}$$

The approximation used is shown below. Note that $0 \le e \le 1$ where $e = 1$ is the case for a black body. The relationship between α and e given in equation C.8, σ_B is the constant in Boltzmann's equation.

$$\begin{cases} T(x) = T_0(x) + \Delta T(x) \\ T^4(x) = T_0^4(x) + 4 \cdot T_0(x)^3 \cdot \Delta T(x) + 6 \cdot T_0(x)^2 \cdot \Delta T(x)^2 + 4 \cdot T_0(x) \cdot \Delta T(x)^3 + \Delta T(x)^4 \end{cases} \Rightarrow$$
$$T^4(x) \approx T_0^4(x) + 4 \cdot T_0(x)^3 \cdot \Delta T(x)$$

$$\begin{cases} k \cdot \frac{\partial T(x)}{\partial x} = e \cdot \sigma_B \cdot \left(T^4(x) - T_0^4(x)\right) \\ T^4(x) \approx T_0^4(x) + 4 \cdot T_0(x)^3 \cdot \Delta T(x) \end{cases} \Rightarrow$$
$$k \cdot \frac{\partial T(x)}{\partial x} \approx e \cdot \sigma_B \cdot \left(T_0^4(x) + 4 \cdot T_0(x)^3 \cdot \Delta T(x) - T_0^4(x)\right) \Leftrightarrow$$
$$k \cdot \frac{\partial T(x)}{\partial x} \approx e \cdot \sigma_B \cdot 4 \cdot T_0^{\,3}(x) \cdot \Delta T(x) \Leftrightarrow$$
$$k \cdot \frac{\partial T(x)}{\partial x} \approx e \cdot \sigma_B \cdot 4 \cdot T_0^{\,3}(x) \cdot (T(x) - T_0(x)) \Leftrightarrow$$
$$\begin{cases} k \cdot \frac{\partial T(x)}{\partial x} \approx \alpha \cdot (T(x) - T_0(x)) \\ \alpha = e \cdot \sigma_B \cdot 4 \cdot T_0^{\,3}(x) \end{cases}$$

$$\alpha = e \cdot \sigma_B \cdot 4 \cdot T_0^{\,3}(x) \tag{C.8}$$

The value of the source term, denoted Ξ, is hard to both measure and derive. With some assumptions and approximations a value which seems reasonable can be calculated. The microwaves heating the carton can be considered to be incident evenly from all angles. Taking the area into account, that means approximately 10 times more microwave power will approach the carton walls compared to the food surface. Due to the similarity between a wave guide and the opening at the top of the carton, the walls get approximately an additional factor 10 more power. Since the depth of penetration is smaller than the thickness of the materials all waves transmitted into the surfaces can be considered absorbed. The largest difference is that most of the incident power is reflected at the metal surface while a fair share of the waves penetrate the food surface. The ratio between the transmitted field power and the incident field power can be calculated with equation C.10, with the use of equation C.9. The derivation of equation C.10 can be made with simple field theory. Summarizing all the properties gives a value in order of $2 \cdot 10^{-2}$. Given the power the microwave oven generates two percent heat the carton walls rather than the food. Dividing that power with the total volume of the metal foil gives an approximate value that can be used as Ξ. Other more accurate calculations for Ξ are possible, but this method has the advantage of being simple and only using basic relations without tedious derivations.

$$\eta = \sqrt{\frac{j \cdot \omega \cdot \mu_{\mathrm{r}} \cdot \mu_0}{j \cdot \omega \cdot \varepsilon_{\mathrm{r}} \cdot \varepsilon_0 + \sigma}} \tag{C.9}$$

$$\frac{P_t}{P_i} = \frac{4 \cdot |\eta_2|^2 \cdot \mathrm{Re}(\eta_2)}{|\eta_1 + \eta_2|^2 \cdot \mathrm{Re}(\eta_1)} \tag{C.10}$$

Appendix D

Pictures

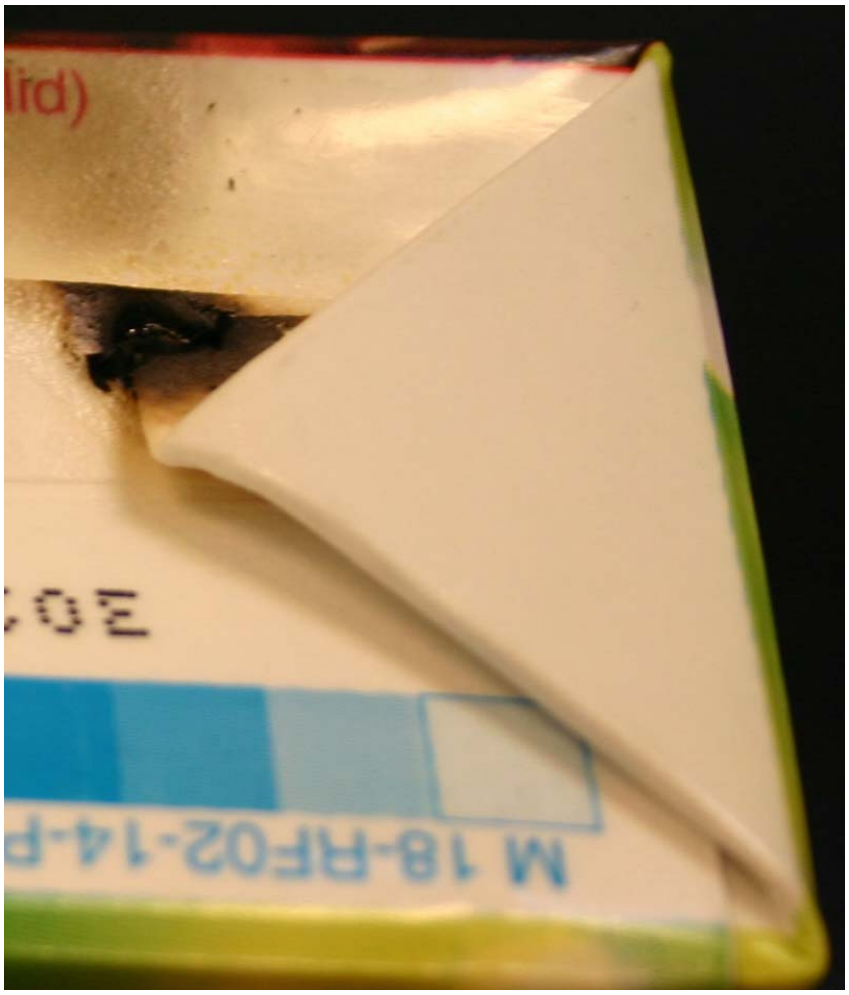

Figure D.1. An ordinary carton where ionization has left burn marks.

Appendix E

Symbols

Symbol	Quantity or name	Unit or value
B	Magnetic flux density	Wb/m^2
c	The speed of light in vacuum	$\approx 3 \cdot 10^8$ m/s
d	Distance	m
D	Electric flux density	C/m^2
D_p	Depth of penetration	m
e	Emission factor	-
E	Electric field	V/m (vector)
E	Electric field component	V/m (scalar)
f	Frequency	Hz
H	Magnetic field	A/m (vector)
H	Magnetic field component	A/m (scalar)
J	Electric current density	A/m^2 (vector)
J	Electric current density component	A/m^2 (scalar)
k	Specific heat	J/(kg·K)
k_t	Transversal wave number	rad/m
k_σ	Thermal conductivity	W/(m·K)
m	Mass	kg
M	Magnetic current density	V/m^2 (vector)
M	Magnetic current density component	V/m^2 (scalar)
p	Pressure	Pa
SAR	Specific Absorption Rate	W/kg
t	Time	s
T	Temperature	K
v	Velocity	m/s
α	Emissivity	$W/(m^2 \cdot K)$
α_{ion}	Number of ionization collisions	m^{-1}
γ	Propagation constant	m^{-1}
γ_{ion}	Number of electrons released	-
ε_0	Permittivity	$\approx 8.85 \cdot 10^{-12}$ F/m
ε_r	Relative permittivity	-
η	Wave impedance	Ω
η_{ion}	Number of attachment collisions	m^{-1}
λ	Wavelength	m
μ_0	Permeability	$\approx 1.26 \cdot 10^{-6}$ H/m
μ_r	Relative permeability	-
Ξ	Power density	W/m^3
ρ	Charge density	C/m^3

σ	Electric conductivity	$\Omega^{-1}\cdot m^{-1}$
σ^*	Magnetic conductivity	Ω/m
σ_B	The constant in Boltzmann's equation	$\approx 5.67\cdot 10^{-8}$ W/($m^2\cdot K^4$)
ω	Angular frequency	rad/s

Table E.1. The symbols stated are used to represent values of either physical quantities or physical constants. Note that a few empirical constants have been left out. Values for these constants can be found in the reference related to the equation they are used in.